

## Geometry and Nanolength Scales versus Interface Interactions: Water Dynamics in AOT Lamellar Structures and Reverse Micelles

David E. Moilanen, Emily E. Fenn, Daryl Wong, and M. D. Fayer\*

*Department of Chemistry, Stanford University, Stanford, California 94305*

Received March 12, 2009; E-mail: fayer@stanford.edu

**Abstract:** To determine the relative importance of the confining geometry and nanoscopic length scale versus water/interface interactions, the dynamic interactions between water and interfaces are studied with ultrafast infrared spectroscopy. Aerosol OT (AOT) is a surfactant that can form two-dimensional lamellar structures with known water layer thickness as well as well-defined monodispersed spherical reverse micelles of known water nanopool diameter. Lamellar structures and reverse micelles are compared based on two criteria: surface-to-surface dimensions to study the effect of confining length scales, and water-to-surfactant ratio to study water/interface interactions. We show that the water-to-surfactant ratio is the dominant factor governing the nature of water interacting with an interface, not the characteristic nanoscopic distance. The detailed structure of the interface and the specific interactions between water and the interface also play a critical role in the fraction of water molecules influenced by the surface. A two-component model in which water is separated into bulk-like water in the center of the lamellar structure or reverse micelle and interfacial water is used to quantitatively extract the interfacial dynamics. A greater number of perturbed water molecules are present in the lamellar structures as compared to the reverse micelles due to the larger surface area per AOT molecule and the greater penetration of water molecules past the sulfonate head groups in the lamellar structures.

### I. Introduction

Water in chemical and biological systems frequently occurs in very crowded environments where the characteristic length scale associated with the environments is nanometers. The important question arises; what is the dominant effect in confined aqueous systems? Is it the geometry of the system with some nanolength scale determined by a surface-to-surface distance that plays the principal role in disrupting the hydrogen bonding network and altering the dynamics of the confined water? Or, is it the water/interface interactions and the relatively static presence of the surface that is the primary influence on water dynamics? Here we answer these questions and show that the nanolength scale is of less significance and that the short-range water/interface interactions are of principal importance.

There is evidence that suggests that both length scale and interface interactions alter water dynamics in confined environments. Surface force and shear measurements on water confined down to a few molecular layers between atomically smooth mica sheets indicate that the structure and properties of water are modified when confined to these length scales.<sup>1,2</sup> Molecular dynamics (MD) simulations of water confined between hydrophobic plates<sup>3</sup> or inside carbon nanotubes<sup>4</sup> also show that modifications occur in the water structure and dynamics. At the

same time, MD simulations have shown that the most strongly perturbed water molecules in a reverse micelle<sup>5</sup> or at the surface of a lipid bilayer<sup>6,7</sup> are the water molecules that are directly in contact with the surface. Magnetic relaxation dispersion (MRD) experiments and MD simulations of protein hydration water in dilute systems show that only the water molecules interacting directly with the surface have strongly perturbed dynamics compared to bulk water.<sup>8–12</sup>

What is it about an interface that slows the orientational dynamics of water? We focus here on orientational relaxation because complete orientational randomization requires concerted rearrangement of the water hydrogen bonding network.<sup>13,14</sup> Therefore, observations of orientational relaxation are closely related to the hydrogen bond network's structural evolution. Are hydrogen bonding interactions so strong that water molecules simply cannot reorient? MD simulations of water around aqueous ions and hydrophobic molecules may provide an answer

(1) Zhu, Y.; Granick, S. *Phys. Rev. Lett.* **2001**, *87*, 096101–096104.

(2) Raviv, U.; Perkin, S.; Laurat, P.; Klein, J. *Langmuir* **2004**, *20*, 5322–5332.

(3) Meyer, M.; Stanley, H. E. *J. Phys. Chem. B* **1999**, *103*, 9728–9730.

(4) Kolesnikov, A. I.; Zanotti, J.-M.; Loong, C.-K.; Thiagarajan, P.; Moravsky, A. P.; Loutfy, R. O.; Burnham, C. J. *Phys. Rev. Lett.* **2004**, *93*, 035501–035504.

(5) Faeder, J.; Ladanyi, B. M. *J. Phys. Chem. B* **2000**, *104*, 1033–1046.

(6) Bhide, S. Y.; Berkowitz, M. L. *J. Chem. Phys.* **2006**, *125*, 094711–094717.

(7) Lopez, C.; Nielsen, S. O.; Klein, M. L.; Moore, P. B. *J. Phys. Chem. B* **2004**, *108*, 6603–6610.

(8) Halle, B. *Philos. Trans. R. Soc. London, Ser. B* **2004**, *359*, 1207–1224.

(9) Halle, B.; Davidovic, M. *Proc. Natl. Acad. Sci. U.S.A.* **2003**, *100*, 12135–12140.

(10) Modig, K.; Liepinsh, E.; Otting, G.; Halle, B. *J. Am. Chem. Soc.* **2004**, *126*, 102–114.

(11) Bagchi, B. *Chem. Rev.* **2005**, *105*, 3197–3219.

(12) Jana, B.; Pal, S.; Bagchi, B. *J. Phys. Chem. B* **2008**, *112*, 9112–9117.

(13) Laage, D.; Hynes, J. T. *Science* **2006**, *311*, 832–835.

(14) Laage, D.; Hynes, J. T. *J. Phys. Chem. B* **2008**, *112*, 14230–14242.

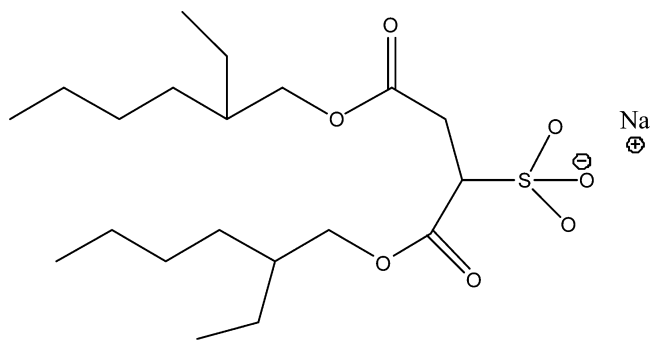


Figure 1. Structure of Aerosol OT.

to this question, indicating that the primary factor that slows water reorientation is the excluded volume effect of the solute that blocks new hydrogen bond acceptors from entering the hydration shell of the reorienting water molecule, not anomalously strong hydrogen bonds.<sup>15,16</sup> The same effect is likely to influence the dynamics at an interface. While a great deal of work has been devoted to understanding the structure and dynamics of water in confined environments and near surfaces, the issue of geometry and length scale versus water/interface interactions has not been experimentally resolved.

The goal of the present work is to systematically study the effects of changing the nanolength scale and geometry of a confining system while keeping the molecular nature of the interface constant. To do this, we employ the surfactant Aerosol OT (AOT), which forms well-characterized, monodispersed reverse micelles in isoctane over a wide range of length scales.<sup>17</sup> Reverse micelles are often characterized by the  $w_0$  parameter, which is defined as the number of water molecules per surfactant molecule,  $w_0 = [\text{H}_2\text{O}]/[\text{AOT}]$ . The radius of the reverse micelle scales with  $w_0$  and can range from less than 1 nm up to 14 nm. AOT also forms lamellar structures when mixed with water, and the lamellar repeat distances have been characterized by X-ray diffraction.<sup>18–20</sup> The lamellar repeat distance scales linearly with the reciprocal of the AOT volume fraction.<sup>18,19</sup> To make the comparison between the lamellar structures and the reverse micelles clear and to differentiate between the two systems, the parameter,  $\lambda$ , will be used to represent the number of water molecules per surfactant in the lamellar structures,  $\lambda = [\text{H}_2\text{O}]/[\text{AOT}]$ .

The structure of AOT is shown in Figure 1. It consists of a sulfonate head group and sodium counterion that preferentially partition into the polar phase. Near the head group on each of the alkyl tails are ester moieties that may also interact with the polar phase depending on the packing and configuration of the AOT molecules. The alkyl tails are branched and bulky; their steric interactions with one another and the nonpolar phase help stabilize the shape of the reverse micelle and play an important role in determining the surface area per AOT molecule in both the reverse micelle and lamellar phases.

The dynamics of water in AOT reverse micelles have been studied extensively by a variety of techniques including

NMR,<sup>21,22</sup> fluorescence,<sup>23–27</sup> neutron scattering,<sup>28</sup> MD simulations,<sup>5,29</sup> and ultrafast infrared spectroscopy.<sup>30–42</sup> All of these studies point to a slowing of the water dynamics as the reverse micelle size decreases. Recently, the orientational relaxation time of interfacial water in AOT reverse micelles has been determined by a detailed investigation of the wavelength-dependent vibrational population relaxation and orientational dynamics of water in large reverse micelles.<sup>42</sup>

AOT reverse micelles have been studied extensively, but much less is known about the dynamics of water in AOT lamellar structures. Most studies have focused on understanding the structure of the lamellar phase. The lamellar repeat distance has been determined by X-ray diffraction,<sup>18,19</sup> the surfactant hydration has been studied by differential scanning calorimetry (DSC),<sup>43</sup> and the infrared spectrum of the confined water has been measured at various hydration levels.<sup>19</sup> Dynamical measurements have primarily been performed using NMR to measure the characteristic length scales for water diffusion,<sup>44–46</sup> but the nature of the interfacial water dynamics and the details of the water/interface interactions are largely unknown. The present work provides a detailed investigation of the dynamics of interfacial water in both AOT lamellar structures and reverse

- (15) Laage, D.; Hynes, J. T. *J. Phys. Chem. B* **2008**, *112*, 7697–7701.  
 (16) Laage, D.; Stirnemann, G.; Hynes, J. T. *J. Phys. Chem. B* **2009**, *113*, 2428–2435.  
 (17) Zulauf, M.; Eicke, H.-F. *J. Phys. Chem.* **1979**, *83*, 480–486.  
 (18) Fontell, K. *J. Colloid Interface Sci.* **1973**, *44*, 318–329.  
 (19) Boissiere, C.; Brubach, J. B.; Mermet, A.; de Marzi, G.; Bourgaux, C.; Prouzet, E.; Roy, P. *J. Phys. Chem. B* **2002**, *106*, 1032–1035.  
 (20) Nallet, F.; Lavessanne, R.; Roux, D. *J. Phys. II* **1993**, *3*, 487–502.

- (21) Grigolini, P.; Maestro, M. *Chem. Phys. Lett.* **1986**, *123*, 248–252.  
 (22) Quist, P.-O.; Halle, B. *J. Chem. Soc., Faraday Trans. 1* **1988**, *84*, 1033–1046.  
 (23) Pant, D.; Riter, R. E.; Levinger, N. E. *J. Chem. Phys.* **1998**, *109*, 9995–10003.  
 (24) Riter, R. E.; Willard, D. M.; Levinger, N. E. *J. Phys. Chem. B* **1998**, *102*, 2705–2714.  
 (25) Douhal, A.; Angulo, G.; Gil, M.; Organero, J. A.; Sanz, M.; Tormo, L. *J. Phys. Chem. B* **2007**, *111*, 5487–5493.  
 (26) Ueda, M.; Schelly, Z. A. *Langmuir* **1989**, *5*, 1005–1008.  
 (27) Zinsli, P. E. *J. Phys. Chem.* **1979**, *83*, 3223–3226.  
 (28) Harpham, M. R.; Ladanyi, B. M.; Levinger, N. E.; Herwig, K. W. *J. Chem. Phys.* **2004**, *121*, 7855–7868.  
 (29) Abel, S.; Sterpone, F.; Bandyopadhyay, S.; Marchi, M. *J. Phys. Chem. B* **2004**, *108*, 19458–19466.  
 (30) Seifert, G.; Patzlaff, T.; Graener, H. *Phys. Rev. Lett.* **2002**, *88*, 147402.  
 (31) Moilanen, D. E.; Levinger, N.; Spry, D. B.; Fayer, M. D. *J. Am. Chem. Soc.* **2007**, *129*, 14311–14318.  
 (32) Piletic, I.; Moilanen, D. E.; Spry, D. B.; Levinger, N. E.; Fayer, M. D. *J. Phys. Chem. A* **2006**, *110*, 4985–4999.  
 (33) Piletic, I.; Tan, H.-S.; Moilanen, D. E.; Spry, D. B.; Fayer, M. D. In *Femtochemistry VII: Fundamental Ultrafast Processes in Chemistry, Physics, and Biology*; Castleman, A. W., Kimble, M. L., Eds.; Elsevier: Amsterdam, 2006; pp 195–203.  
 (34) Piletic, I. R.; Tan, H.-S.; Fayer, M. D. *J. Phys. Chem. B* **2005**, *109*, 21273–21284.  
 (35) Tan, H.-S.; Piletic, I. R.; Fayer, M. D. *J. Chem. Phys.* **2005**, *122*, 174501–174509.  
 (36) Tan, H.-S.; Piletic, I. R.; Riter, R. E.; Levinger, N. E.; Fayer, M. D. *Phys. Rev. Lett.* **2005**, *94*, 057405.  
 (37) Tan, H.-S.; Piletic, I. R.; Riter, R. E.; Levinger, N. E.; Fayer, M. D. *Phys. Rev. Lett.* **2004**, *94*, 057405–057404.  
 (38) Dokter, A. M.; Woutersen, S.; Bakker, H. J. *Phys. Rev. Lett.* **2005**, *94*, 178301.  
 (39) Dokter, A. M.; Woutersen, S.; Bakker, H. J. *Proc. Natl. Acad. Sci. U.S.A.* **2006**, *103*, 15355–15358.  
 (40) Cringus, D.; Bakulin, A.; Lindner, J.; Vohringer, P.; Pshenichnikov, M. S.; Wiersma, D. A. *J. Phys. Chem. B* **2007**, *111*, 14193–14207.  
 (41) Cringus, D.; Lindner, J.; Milder, M. T. W.; Pshenichnikov, M. S.; Vohringer, P.; Wiersma, D. A. *Chem. Phys. Lett.* **2005**, *408*, 162–168.  
 (42) Moilanen, D. E.; Fenn, E. E.; Wong, D.; Fayer, M. D. *J. Phys. Chem. B*, in press.  
 (43) Casillas, N.; Puig, J. E.; Olayo, R.; Hart, T. J.; Franses, E. I. *Langmuir* **1989**, *5*, 384–389.  
 (44) Aslund, I.; Cabaleiro-Lago, C.; Soderman, O.; Topgaard, D. *J. Phys. Chem. B* **2008**, *112*, 2782–2794.  
 (45) Callaghan, P. T.; Soderman, O. *J. Phys. Chem.* **1983**, *87*, 1737–1744.  
 (46) Hubbard, P. L.; McGrath, K. M.; Callaghan, P. T. *J. Phys. Chem. B* **2006**, *110*, 20781–20788.

micelles to study the effects of confining length scales, geometry, and water/interface interactions on the dynamics of water.

To address the question of length scale, lamellar structures that have the same water layer thickness as a given reverse micelle's diameter are compared. This comparison allows the effect of surface-to-surface distance in two-dimensional versus three-dimensional confined systems to be determined. The effect of water/interface interactions is addressed by preparing reverse micelles and lamellar structures that have the same number of water molecules per AOT molecule. It has been shown by DSC that the number of unfreezable water molecules is the same for AOT lamellar structures and reverse micelles, indicating that the head group/water interactions are similar in the two systems.<sup>43,47</sup> One major difference between the reverse micelles and the lamellar structures is the surface area per AOT molecule.<sup>18,48</sup> Due to the steric interactions of the alkyl tails and the differences in the curvature of the spherical reverse micelle and the planar lamellar surfaces, the surface area per AOT is significantly larger in the lamellar structures. This difference is shown to be important, demonstrating how variations in surface topography play a significant role in governing the number of perturbed water molecules. In spite of the differences in geometry and topography, we show that the water/interface interactions are very similar in the reverse micelle and lamellar systems and that the dynamics of the confined water are affected most strongly by direct interaction with the interface as opposed to longer-range effects where the nanoscopic length scale and the spherical versus planar geometry would play significant roles.

## II. Experimental Procedures

Aerosol OT (sodium bis(2-ethylhexyl) sulfosuccinate), isooctane, H<sub>2</sub>O, and D<sub>2</sub>O (Aldrich, Inc.) were used as received. A 0.5 M stock solution of AOT in isooctane was prepared, and the residual water content in the stock solution was determined by Karl Fischer titration to be 0.5 water molecules per AOT ( $w_0 = 0.5$ ). A stock solution of 5% HOD in H<sub>2</sub>O was added to measured amounts of the 0.5 M stock solution to prepare reverse micelles with the desired  $w_0$ . Reverse micelle sizes for a given  $w_0$  have been determined by photon correlation spectroscopy<sup>17</sup> and viscosity measurements.<sup>49</sup> Lamellar structures were prepared by adding water to dry AOT to produce samples with various water-to-surfactant ratios,  $\lambda$ . The water thickness of lamellar samples of varying water to surfactant ratios has been determined by X-ray diffraction.<sup>18,19</sup> Four lamellar structures were prepared,  $\lambda = 16.5, 25, 37,$  and  $46$  with water layer thicknesses of  $1.6, 2.3, 3.3,$  and  $4.0$  nm, respectively. Eight sizes of reverse micelles were prepared for comparison with the lamellar structures. To compare the surface-to-surface distances, reverse micelles of  $w_0 = 2, 5, 7.6,$  and  $10$  were prepared with diameters of  $1.6, 2.3, 3.3,$  and  $4.0$  nm, respectively. The other four reverse micelles have the same water-to-surfactant ratio as the lamellar structures,  $w_0 = 16.5, 25, 37,$  and  $46$  with diameters of  $5.8, 9.0, 17,$  and  $20$  nm, respectively.

Samples for infrared absorption and ultrafast IR experiments were housed in copper sample cells between two CaF<sub>2</sub> windows separated by a Teflon spacer. The thickness of the spacer was selected to maintain an optical density of  $\sim 0.5$  in the OD stretch region for all samples. The OD stretch of dilute HOD in H<sub>2</sub>O is used to eliminate problems due to vibrational excitation transfer that can

cause artificial decay of the orientational correlation function.<sup>50,51</sup> MD simulations of HOD in bulk H<sub>2</sub>O demonstrate that dilute HOD does not change the properties of water, and the dynamics of HOD report on the dynamics of water.<sup>52</sup>

The laser system used for these experiments consists of a Ti:sapphire oscillator and regenerative amplifier pumping an OPA and difference frequency stage to produce  $\sim 70$  fs pulses at  $\sim 4 \mu\text{m}$  ( $2500 \text{ cm}^{-1}$ ). The mid-IR light was split into an intense pump pulse and a weak probe pulse. Before the sample, the polarization of the pump pulse is rotated from horizontal to  $45^\circ$  relative to the horizontally polarized probe. The pump pulse is passed through a polarizer set to  $45^\circ$  immediately before the sample to ensure that the HOD molecules are excited by a linearly polarized pump pulse. The polarization of the probe is resolved parallel and perpendicular ( $+45^\circ$  and  $-45^\circ$  relative to horizontal) to the pump after the sample using a computer-controlled rotation stage. Another polarizer immediately after the resolving polarizer and just before the input to the monochromator is used to set the polarization entering the monochromator to horizontal to eliminate differences in the polarization-dependent reflection and diffraction efficiencies in the monochromator.<sup>53</sup> The probe is frequency dispersed by the monochromator and detected using a 32 element MCT detector (Infrared Associates and Infrared Systems Design).

The pump-probe signal measured parallel ( $I_{\parallel}$ ) and perpendicular ( $I_{\perp}$ ) to the pump contains information about both the population relaxation and the orientational dynamics of the HOD molecules.<sup>54</sup>

$$I_{\parallel} = P(t)(1 + 0.8C_2(t)) \quad (1)$$

$$I_{\perp} = P(t)(1 - 0.4C_2(t)) \quad (2)$$

$P(t)$  is the vibrational population relaxation, and  $C_2(t)$  is the second Legendre polynomial orientational correlation function. Pure population relaxation can be extracted from the parallel and perpendicular signals using

$$P(t) = I_{\parallel} + 2I_{\perp} \quad (3)$$

In the case of a single ensemble of molecules undergoing orientational relaxation, the orientational correlation function,  $C_2(t)$ , can be determined from the anisotropy,  $r(t)$ , by

$$r(t) = (I_{\parallel} - I_{\perp})/(I_{\parallel} + 2I_{\perp}) = 0.4C_2(t) \quad (4)$$

The additional complications that arise in calculating the anisotropy when two distinct subensembles of molecules exist in the system will be discussed in detail below.

## III. Results and Discussion

**A. Nanoscopic Length or Water/Interface Interactions? 1. Infrared Spectra.** The OD stretching mode of HOD in H<sub>2</sub>O is sensitive to the local hydrogen bonding network structure of water as well as the local electric fields acting on the OD bond.<sup>55,56</sup> Infrared spectra of the OD stretch of water in reverse micelles and lamellar structures can provide information about

(47) Hauser, H.; Haering, G.; Pande, A.; Luisi, P. L. *J. Phys. Chem.* **1989**, *93*, 7869–7876.

(48) Eicke, H.-F.; Rehak, J. *Helv. Chim. Acta* **1976**, *59*, 2883–2891.

(49) Kinugasa, T.; Kondo, A.; Nishimura, S.; Miyauchi, Y.; Nishii, Y.; Watanabe, K.; Takeuchi, H. *Colloids Surf., A* **2002**, *204*, 193–199.

(50) Woutersen, S.; Bakker, H. J. *Nature* **1999**, *402*, 507–509.

(51) Gaffney, K. J.; Piletic, I. R.; Fayer, M. D. *J. Chem. Phys.* **2003**, *118*, 2270–2278.

(52) Asbury, J. B.; Steinel, T.; Kwak, K.; Corcelli, S. A.; Lawrence, C. P.; Skinner, J. L.; Fayer, M. D. *J. Chem. Phys.* **2004**, *121*, 12431–12446.

(53) Tan, H.-S.; Piletic, I. R.; Fayer, M. D. *J. Opt. Soc. Am. B* **2005**, *22*, 2009–2017.

(54) Tokmakoff, A. *J. Chem. Phys.* **1996**, *105*, 1–12.

(55) Smith, J. D.; Cappa, C. D.; Wilson, K. R.; Cohen, R. C.; Geissler, P. L.; Saykally, R. J. *Proc. Natl. Acad. Sci. U.S.A.* **2005**, *102*, 14171–14174.

(56) Smith, J. D.; Saykally, R. J.; Geissler, P. L. *J. Am. Chem. Soc.* **2007**, *129*, 13847–13856.

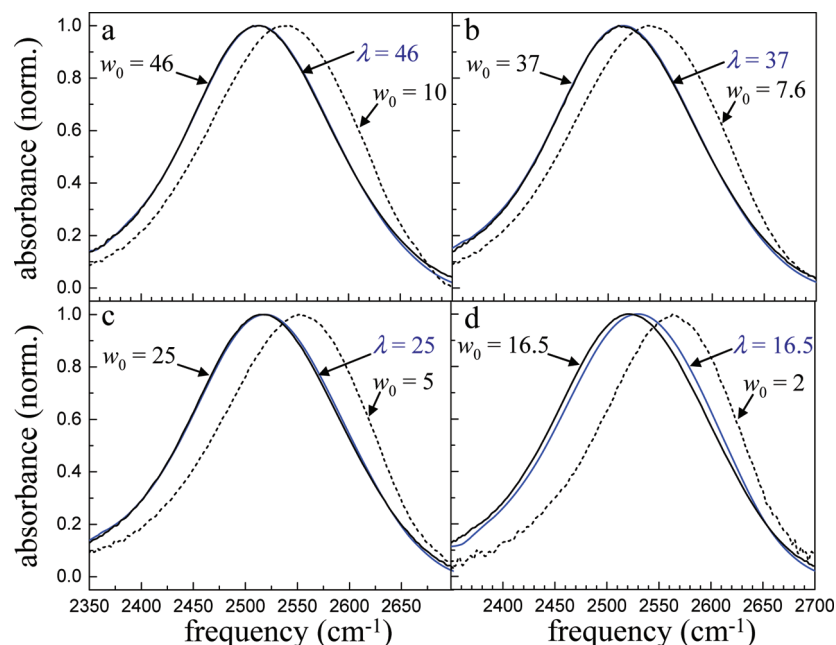


**Figure 2.** Normalized infrared absorption spectra of the OD stretch of dilute HOD in H<sub>2</sub>O in AOT lamellar structures and reverse micelles. Lamellar structures: blue curves. Large reverse micelles with  $w_0 = \lambda$ : solid black curves. Small reverse micelles with the same characteristic nanoscopic distance as the lamellar structure (diameter vs interplanar distance): dashed black curves.

these two factors. Figure 2 shows the infrared absorption spectra of the four lamellar structures and eight reverse micelles. Each panel of Figure 2 groups the spectrum of a lamellar structure with two reverse micelle spectra.

The two reverse micelle spectra are the spectrum of the reverse micelle that has the same diameter as the surface-to-surface distance of the lamellar structure and the spectrum of the reverse micelle that has the same number of water molecules per AOT,  $w_0 = \lambda$ . It is clear in Figure 2 that the spectra of the lamellar structures are much more similar to the spectra of the reverse micelles that have  $w_0 = \lambda$ . The important point is that the characteristic nanoscopic dimension of the system is not the dominant influence on the spectra.

The fact that the hydroxyl stretch spectra do not depend on the nanoscopic size of the system at least for larger nanoscopic dimensions is not too surprising because the absorption frequency is determined by very local interactions. It has been shown that the IR spectrum of water in reverse micelles shifts progressively to higher frequencies in a monotonic fashion as the reverse micelle size, or  $w_0$ , decreases.<sup>32,42</sup> In fact, the spectrum can be modeled as a linear combination of the spectrum of bulk water (peak at 2509 cm<sup>-1</sup>) and the spectrum of the  $w_0 = 2$  reverse micelle (peak at 2565 cm<sup>-1</sup>).<sup>32</sup> The infrared spectrum of the hydroxyl stretch in bulk water is sensitive to the hydrogen bond strength and the number of hydrogen bonds.<sup>57</sup> In reverse micelles and lamellar structures, it is unclear whether the shift in the spectrum to higher frequencies should be attributed to different hydrogen bonding interactions with the interface or to the electric fields caused by the anionic sulfonate groups and cationic sodium counterions as has recently been suggested.<sup>56</sup> In either case, it is clear from the IR spectrum that the hydrogen bonding environment in the lamellar structures is not dominated by the surface-to-surface distance, but instead by the specific water/interface interactions.

While on a coarse level the water/interface interactions dominate the IR spectrum, the specific nature of the water/interface interactions does not strictly depend on the number of waters per AOT. This is particularly evident in Figure 2d that shows a comparison between the reverse micelle and lamellar structure with 16.5 waters per AOT. The IR spectrum of the lamellar structure is somewhat shifted to higher frequencies relative to the reverse micelle spectrum. This shows that, while similar, the water/interface interactions are not identical in the two structures in spite of the fact that the chemical composition of the interface is the same. These differences in the properties of water in reverse micelles and lamellar structures with  $w_0 = \lambda$  are even more apparent in the vibrational population relaxation results discussed below.

**2. Vibrational Population Relaxation.** Vibrational population relaxation is very sensitive to variations in the local environment of the water molecule.<sup>32,58,59</sup> In the ultrafast pump-probe experiments described here, we excite the 0→1 vibrational transition of the OD stretch. This excitation will decay by pathways involving other modes in the system. Energy must be conserved. The initially excited OD stretch decays into a combination of lower frequency modes that have energies that sum to the original OD vibrational energy.<sup>58</sup> These pathways include high frequency modes of the excited water molecule, such as bends, high frequency modes of other molecules (water or AOT) and low frequency bath modes, such as torsional and translational modes.<sup>32,60</sup> Because several discrete intramolecular modes are unlikely to match the energy of the initially excited mode, creation or annihilation of one or more modes of the continuum is necessary to conserve energy.<sup>58</sup> The OD stretch in different structural environments will have different coupled intramolecular modes and will experience a different density of states of the continuum. Small changes in the lower frequency

(58) Kenkre, V. M.; Tokmakoff, A.; Fayer, M. D. *J. Chem. Phys.* **1994**, *101*, 10618–10629.

(59) Egorov, S. A.; Skinner, J. L. *J. Chem. Phys.* **2000**, *112*, 275–281.

(60) Egorov, S. A.; Berne, B. J. *J. Chem. Phys.* **1997**, *107*, 6050–6061.

(57) Corcelli, S.; Skinner, J. L. *J. Phys. Chem. A* **2005**, *109*, 6154–6165.

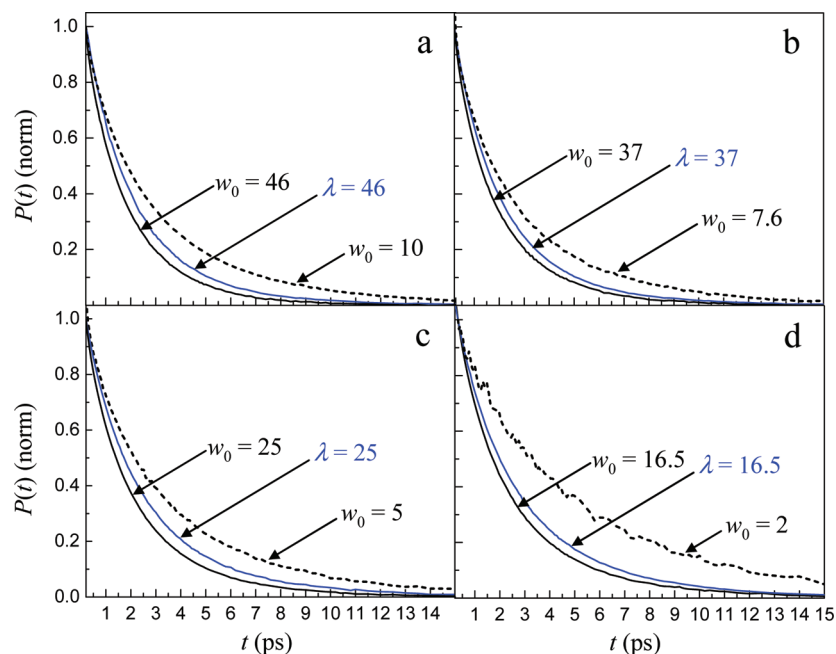


**Figure 3.** Normalized vibrational population relaxation decays at  $2548\text{ cm}^{-1}$  in the lamellar structures and reverse micelles. Lamellar structures: blue curves. Large reverse micelles with  $w_0 = \lambda$ : solid black curves. Small reverse micelles with the same characteristic nanoscopic distance as the lamellar structure (diameter vs interplanar distance): dashed black curves.

bath modes that may not affect the OD stretching frequency can frustrate vibrational relaxation. Therefore, the lifetime is very sensitive to the local environment.<sup>32</sup>

The vibrational population relaxation data at  $2548\text{ cm}^{-1}$  of water in the lamellar structures and corresponding reverse micelles are shown in Figure 3. The data have been corrected for a small, well-documented isotropic heating contribution.<sup>61,62</sup> Again, it is clear that the vibrational relaxation in the lamellar structures is more similar to the reverse micelles that have  $w_0 = \lambda$  as opposed to the reverse micelles with diameters that match

the interplanar spacing of the lamellae. Clearly, the water/interface interactions are the dominant effect, yet in Figure 3, the differences between the reverse micelles and lamellar structures with  $w_0 = \lambda$  are evident. The vibrational lifetimes in the lamellar structures appear to be slower than they are in the reverse micelles of corresponding  $w_0$ . As we will see in section III.C below, the differences are not actually caused by intrinsically slower vibrational lifetimes, but by a larger fraction of the water molecules interacting with the interface in the lamellar structures than in the reverse micelles. The decays are a

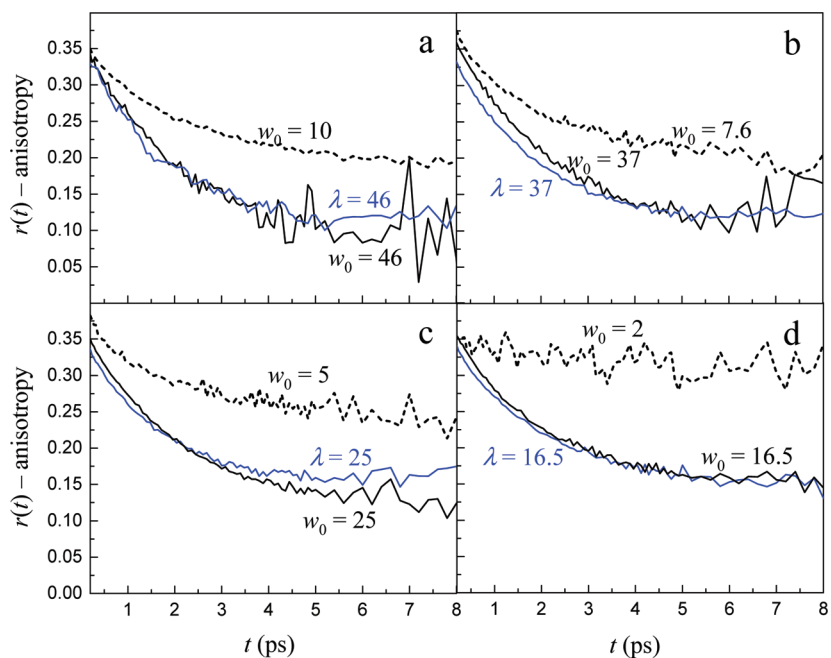


**Figure 4.** Anisotropy decay curves at  $2548\text{ cm}^{-1}$  for the lamellar structures and reverse micelles. Lamellar structures: blue curves. Large reverse micelles with  $w_0 = \lambda$ : solid black curves. Small reverse micelles with the same characteristic nanoscopic distance as the lamellar structure (diameter vs interplanar distance): dashed black curves.

combination of the bulk water decay (fast) and the interfacial water decay (slow). A larger fraction of the water interacts with the lamellar interfaces than with the reverse micelle interfaces, although  $w_0 = \lambda$ . The increase in the magnitudes of the slow components is responsible for the apparent slower decay for the lamellar data.

**3. Orientational Dynamics.** Perhaps the most telling dynamical observable for the nature of water confined in the lamellar structures and reverse micelles is the orientational anisotropy decay. Figure 4 displays the anisotropy decays of the lamellar structures and corresponding reverse micelles at  $2548 \text{ cm}^{-1}$ . On a qualitative level, it is clear once again that the orientational dynamics in the lamellar structures are much more similar to the reverse micelles that have  $w_0 = \lambda$  than to the reverse micelles that have the same diameter as the interplanar separation of the lamellae. These results demonstrate that orientational relaxation, which is directly related to the hydrogen bond network dynamics, is most strongly perturbed for waters directly interacting with a surface, as has been shown recently by a detailed examination of the interfacial water in large reverse micelles.<sup>42</sup> Still, there are differences between the orientational anisotropy decays of the lamellar structures and reverse micelles, just as there were differences in the vibrational lifetimes. In section III.C, the orientational relaxation and vibrational lifetime results will be analyzed quantitatively. It will be shown that the apparent differences in dynamics of water in reverse micelles and lamellae are actually caused by a larger fraction of the water interacting with the interface in the lamellar structures. Water molecules interacting with interfaces in the two geometrically distinct systems share the same characteristic dynamics.

**B. Two-Component Model for Water in Confined Systems.** In the case of a single reorienting ensemble, the anisotropy decay is a measure of the second Legendre polynomial orientational correlation function,  $C_2(t)$  (see eq 4). However, when multiple ensembles are present, the anisotropy decay is more complicated and the decay curves do not directly reflect the orientational dynamics. For a single-component system, as can be seen from eq 4, the denominator divides out the vibrational lifetime. This is no longer true with a two-component system with the components having distinct lifetimes and orientational relaxation dynamics. The issues that arise in interpreting the anisotropy decay for multicomponent systems have been discussed in detail recently.<sup>42</sup>

The problem can be seen clearly by explicitly writing out the numerator and denominator of eq 4 for two components.

$$r(t) = \frac{a(I_{\parallel}^1 - I_{\perp}^1) + (1 - a)(I_{\parallel}^2 - I_{\perp}^2)}{a(I_{\parallel}^1 + 2I_{\perp}^1) + (1 - a)(I_{\parallel}^2 + 2I_{\perp}^2)}$$

$$= 0.4 \frac{aP_1(t)C_2^1(t) + (1 - a)P_2(t)C_2^2(t)}{aP_1(t) + (1 - a)P_2(t)} \quad (5)$$

Here,  $a$  is a weighting factor that represents the fraction of the signal due to component 1. The parallel and perpendicular pump–probe signals due to component  $i$  are given by  $I_{\parallel}^i$  and  $I_{\perp}^i$ , respectively.  $P_i(t)$  is the population relaxation of component  $i$ , and the orientational correlation functions are given by  $C_2^i(t)$ . The interplay of the weighting factor,  $a$ , the two vibrational lifetimes, and orientational correlation functions can lead to nonintuitive decay curves which have been simulated and discussed recently.<sup>42</sup> Unlike the anisotropy decay, the population

relaxation is given simply by a weighted sum of the two components contributing to the signal.

$$P(t) = aP_1(t) + (1 - a)P_2(t) \quad (6)$$

The variables are the same as in eq 5.

While it is clear that the anisotropy decays of the small reverse micelles do not match the lamellar anisotropy decays, a complete understanding of the similarities and differences between the dynamics of water in the reverse micelles and lamellar structures that have  $w_0 = \lambda$  requires a determination of the vibrational relaxation times and orientational relaxation times. To accomplish this goal, we apply a two-component model to simultaneously fit the vibrational population relaxation and anisotropy decays for both the reverse micelles and lamellar structures. Two-component models consisting of a bulk-like core and a shell of interfacial water molecules have been applied previously to analyze the infrared spectra and vibrational lifetimes of water in AOT reverse micelles.<sup>32,40</sup> Recently, it was shown that the orientational dynamics of water in large reverse micelles could also be modeled as consisting of a core of bulk water and a shell of interfacial water, which has a slower vibrational lifetime and orientational relaxation time.<sup>42</sup> The interfacial water in large reverse micelles has a characteristic vibrational lifetime of 4.3 ps and an orientational relaxation time of 18 ps.<sup>42</sup> These recent results are consistent with those obtained previously that set a lower bound of 15 ps for the orientational dynamics of interfacial water when studying the OH stretch of HOD in  $\text{D}_2\text{O}$  in AOT reverse micelles.<sup>39</sup>

In the case of large reverse micelles, it is reasonable to assume that water far from the interface has characteristics similar to bulk water. The extended jump model of Laage and Hynes shows that water reorientation is primarily governed by the availability of new hydrogen bond acceptors in the second solvation shell of a reorienting water molecule.<sup>13,14</sup> A significant amount of the water in the core of a large reverse micelle has a second solvation shell that does not interact with the interface, and these water molecules behave the same as bulk water.

Water molecules interacting with the interface are expected to have slower long time orientational relaxation decays than bulk water. Long time orientational relaxation is associated with processes that contribute to complete orientational randomization. The slowing is due to the presence of the interface that blocks the ability of new hydrogen bond acceptors to move into the solvation shell of the interfacial water.<sup>16</sup> Similar slowing has been observed in ionic solutions<sup>63,64</sup> and around hydrophobic solutes.<sup>65</sup> These interfacial waters have slow complete randomization times but are not static on a short time scale. Instead, they sample a significant range of angular space about their hydrogen bond axis without breaking their hydrogen bonds. The restricted angular sampling is referred to as wobbling-in-a-cone.

An example of wobbling-in-a-cone is given in Figure 5, which shows the anisotropy decays of bulk water as well as water in the  $w_0 = 2$  reverse micelle at two frequencies. The bulk water anisotropy decays as a single exponential with a time constant

(61) Steinel, T.; Asbury, J. B.; Fayer, M. D. *J. Phys. Chem. A* **2004**, *108*, 10957–10964.

(62) Bakker, H. J.; Woutersen, S.; Nienhuys, H. K. *Chem. Phys.* **2000**, *258*, 233–245.

(63) Kropman, M. F.; Bakker, H. J. *J. Chem. Phys.* **2001**, *115*, 8942–8948.

(64) Park, S.; Moilanen, D. E.; Fayer, M. D. *J. Phys. Chem. B* **2008**, *112*, 5279–5290.

(65) Rezus, Y. L. A.; Bakker, H. J. *Phys. Rev. Lett.* **2007**, *99*, 148301–148304.

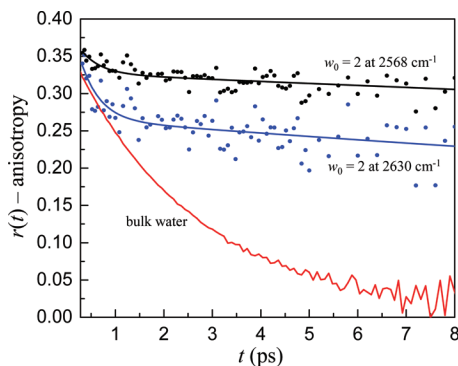


**Figure 5.** Anisotropy decay curves for bulk water (red) and the  $w_0 = 2$  reverse micelle at two frequencies. Bulk water: single exponential with a decay constant of 2.6 ps;  $w_0 = 2$  reverse micelles have a fast wobbling reorientation with a time constant of  $\sim 0.5$  ps followed by very slow orientational relaxation. The higher OD stretching frequency, which corresponds to weaker hydrogen bonds, displays a larger amplitude wobbling component.

of 2.6 ps. In contrast, water in the  $w_0 = 2$  reverse micelle has a very fast reorientation followed by an essentially static offset reflecting orientational relaxation that is too slow to measure within the experimental time scale that is limited by the vibrational lifetime. In the  $w_0 = 2$  reverse micelle, all of the water is either directly interacting with a relatively static sulfonate head group or hydrogen bonded to a water that is interacting with a head group. These interactions with the interface make it very difficult for a water molecule to undergo complete reorientation. In spite of this constraint for complete reorientation, a significant amount of orientational relaxation occurs on a fast time scale, and the amount of reorientational motion is correlated with the OD stretching frequency. In general, higher OD stretching frequencies correspond to weaker hydrogen bonding interactions, and it is apparent that the amplitude of the fast reorientation is larger at  $2630\text{ cm}^{-1}$  than at  $2568\text{ cm}^{-1}$ . This behavior is in agreement with MD simulations that found significant OH bond angular motion in the interfacial region of small reverse micelles even though the reorientation of the entire water molecule was much slower.<sup>5</sup> The trend in fast angular motion is also in agreement with both experimental<sup>66</sup> and simulation<sup>67</sup> results on bulk water that found a larger inertial reorientation for weaker hydrogen bonds that have higher frequency hydroxyl stretch absorptions. In bulk water, hydrogen bond switching events occur rapidly enough that the wobbling motion is not resolvable, but in the  $w_0 = 2$  reverse micelle, the separation of time scales is large and the fast decay is clear. In the interfacial region of large reverse micelles and lamellar structures, this fast wobbling reorientation about the hydrogen bond axis makes an important contribution to the anisotropy decay and must be included to successfully model the dynamics.

Equation 5 has a number of variables, and it would be difficult to extract useful information about the dynamics of interfacial water without fixing some parameters. The most logical parameters to fix are the vibrational lifetime and orientational time of the core waters at the well-known values for bulk water,  $T_{\text{bulk}} = 1.8$  ps and  $\tau_r^{\text{bulk}} = 2.6$  ps, respectively. This approach has worked well for analyzing the dynamics of interfacial water in large reverse micelles.<sup>42</sup> Since the number of water molecules

per head group in the lamellar structures is the same as in the reverse micelles, the same approach will be used here to analyze the dynamics of the interfacial water. The unknown quantities are the population relaxation time of the interfacial water molecules,  $P_{\text{int}}(t)$ , and the orientational correlation function of the interfacial waters,  $C_2^{\text{int}}(t)$ . When the fast wobbling motion is included in the orientational correlation function of the interfacial water molecules,  $C_2^{\text{int}}(t)$  is given by

$$C_2^{\text{int}}(t) = be^{-t/\tau_w} + (1 - b)e^{-t/\tau_r^{\text{int}}} \quad (7)$$

Here,  $\tau_w$  is the time constant for the fast wobbling reorientation. To reduce the number of adjustable parameters, its value was fixed at 0.45 ps to match the time constant for this motion in the  $w_0 = 2$  reverse micelle. The parameter  $b$  is the fractional amplitude of the orientational correlation function due to the wobbling motion, and  $\tau_r^{\text{int}}$  is the time constant for the complete reorientation of interfacial water. In the next section, the two-component model will be applied to the vibrational population relaxation and anisotropy decays of water in the lamellar structures and reverse micelles with  $w_0 = \lambda$  to extract information about the dynamics of the interfacial water in these two systems.

**C. Dynamics of Water near AOT Interfaces.** In a previous work,<sup>42</sup> the spectral region most likely to contain information about water interacting with the interface in large AOT reverse micelles was identified to lie at frequencies higher than  $2565\text{ cm}^{-1}$ . The same spectral region is investigated here to yield information about the dynamics of water near AOT lamellar interfaces. Vibrational lifetimes and anisotropy decays at five frequencies over a range of  $40\text{ cm}^{-1}$  from  $2578$  to  $2619\text{ cm}^{-1}$  are fit simultaneously for each sample. Within this spectral range, we assume that the vibrational lifetime and orientational dynamics of the interfacial water are independent of frequency. The simultaneous fitting results in a characteristic vibrational lifetime and orientational time for interfacial water, a weighting factor  $a$  at each frequency that represents the fraction of the signal due to interfacial water, and a fraction  $b$  that represents the amplitude of the interfacial water orientational correlation function due to fast wobbling reorientation.

Anisotropy decays and the fits from the two-component model are shown for the data at  $2578\text{ cm}^{-1}$  in Figure 6. The fits capture the shapes of the anisotropy curves quite well, and the simultaneous fits to the vibrational lifetime (not shown) are excellent. The quality of the fits demonstrates that the water dynamics are well described by a two-component model consisting of bulk water and slower interfacial water. The fit parameters for the interfacial water dynamics in the AOT lamellar structures and reverse micelles are given in Table 1. Within experimental error, the vibrational lifetimes and long time orientational dynamics in the two systems are the same, with an average vibrational lifetime of  $T_{\text{int}} = 4.3 \pm 0.2$  ps and an average orientational time of  $\tau_r^{\text{int}} = 18 \pm 2$  ps. The results demonstrate that the molecular mechanisms that govern the dynamics of interfacial water are essentially the same in the two systems.

While the anisotropy decays in Figure 6 look fairly similar to one another, they are clearly not identical. Yet the underlying dynamics, including the important long time interfacial water reorientation time, are the same. To understand why the curves appear different, it is instructive to examine the frequency dependence of the fraction of interfacial water,  $a$ , and the wobbling fraction,  $b$ . Table 2 contains the frequency dependence

(66) Moilanen, D. E.; Fenn, E. E.; Lin, Y.-S.; Skinner, J. L.; Bagchi, B.; Fayer, M. D. *Proc. Natl. Acad. Sci. U.S.A.* **2008**, *105*, 5295–5300.  
 (67) Laage, D.; Hynes, J. T. *Chem. Phys. Lett.* **2006**, *433*, 80–85.

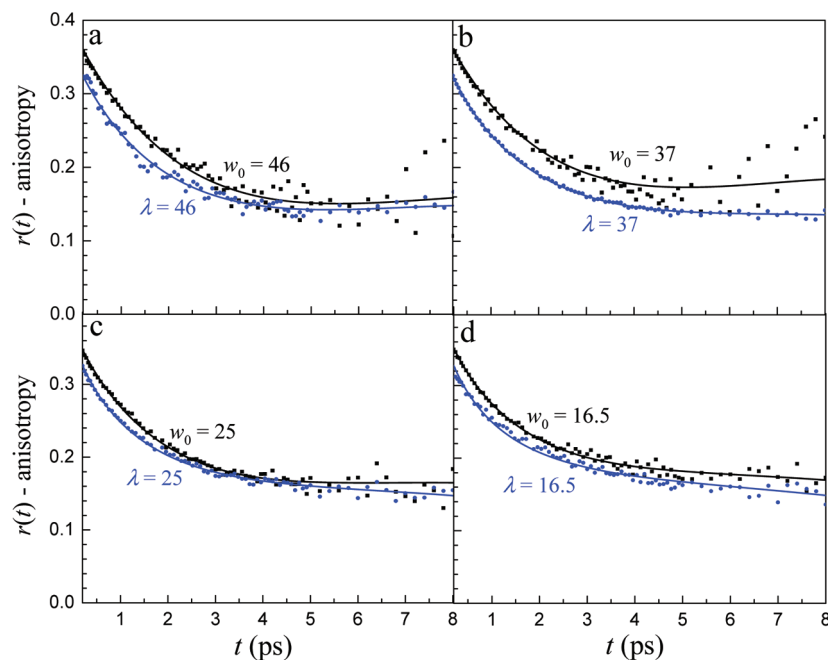


**Figure 6.** Anisotropy decay curves and two-component model fits for the lamellar structures and reverse micelles that have the same number of water molecules per AOT,  $w_0 = \lambda$ . The model describes the data well for all the samples.

**Table 1.** Vibrational Population Relaxation ( $T_{\text{int}}$ ) and Orientational Relaxation ( $\tau_r^{\text{int}}$ )

size <sup>a</sup>	$T_{\text{int}}$ (ps)	$\tau_r^{\text{int}}$ (ps)
$w_0 = 46$	$3.9 \pm 0.5$	$18 \pm 3$
$\lambda = 46$	$4.3 \pm 0.5$	$24 \pm 9$
$w_0 = 37$	$4.6 \pm 0.5$	$18 \pm 3$
$\lambda = 37$	$4.1 \pm 0.3$	$19 \pm 3$
$w_0 = 25$	$4.3 \pm 0.5$	$19 \pm 3$
$\lambda = 25$	$4.2 \pm 0.3$	$18 \pm 2$
$w_0 = 16.5$	$4.4 \pm 0.3$	$17 \pm 3$
$\lambda = 16.5$	$4.5 \pm 0.3$	$17 \pm 2$

<sup>a</sup> Reverse micelle ( $w_0$ ); lamellar ( $\lambda$ ).

of these two factors in the interfacial water spectral region (2578 to 2619  $\text{cm}^{-1}$ ). In the two largest reverse micelles,  $w_0 = 46$  and 37, the contribution to the signal due to interfacial water is small enough that the wobbling amplitude,  $b$ , cannot be resolved. Samples that have an interfacial contribution,  $a$ , greater than 0.2 require fast wobbling to fit the data. Several trends are apparent in data in Table 2. First, for any given sample, the fraction of the signal due to interfacial water becomes larger at higher frequencies. This result is consistent with interfacial waters contributing to the signal at higher frequencies as manifested in the blue shift of the IR spectrum and slowing of the vibrational lifetime when water is confined in progressively smaller reverse micelles.<sup>32,42</sup> The second important trend is that, for samples with the same geometry (reverse micelles or lamellar structures), decreasing the number of water molecules per AOT leads to an increase in the fraction of water molecules interacting with the interface. There are also important trends in the amplitude of the wobbling reorientation,  $b$ . As shown in Figure 5, the amplitude of  $b$  increases as the OD stretching frequency increases. This is associated with a weakening of the OD–O hydrogen bond that allows larger angular excursions around the hydrogen bond axis.

In Table 2, a comparison of the fraction of interfacial water in reverse micelles and lamellar structures with  $w_0 = \lambda$  shows that the single most important factor that makes the curves in

Figure 6 appear different is,  $a$ , the relative amount of interfacial water that contributes to the signal. In all cases, the lamellar structures have a significantly larger contribution due to interfacial water. The larger interfacial water contribution in the lamellae quantitatively explains the vibrational lifetime data in Figure 3. The vibrational lifetime appears to be slower in the lamellar structures because a larger fraction of interfacial water, with its long lifetime, contributes to the signal not because the relaxation mechanisms are different in the two types of samples.

A secondary factor that makes the curves look different is the fraction of the interfacial water orientational correlation function due to fast wobbling,  $b$ . In the lamellar structures,  $b$  is systematically larger than in the reverse micelles. This indicates that the hydrogen bonding network at the interface of AOT lamellar structures allows the OD vector to sample a larger angular range. The curves also look different because the fast inertial drop in the anisotropy,<sup>66</sup> which occurs at shorter times than the wobbling, is larger in the lamellar structures. The inertial drop in bulk water occurs during the first  $\sim 200$  fs and depends on the strength of both the local OD–O hydrogen bond as well as the other hydrogen bonds that a water molecule forms.<sup>66</sup> Moilanen et al. showed that the amplitude of the inertial drop depended not only on the OD stretching frequency of the reorienting water but also on the average distribution of hydrogen bond strengths in the ensemble of water molecules. When hydrogen bonds are on average weaker, the inertial drop is larger. Conversely, stronger average hydrogen bonds restrict the amplitude of the inertial drop.<sup>66</sup> These results indicate that the hydrogen bonding network at the lamellar interface is weaker, on average, than at the reverse micelle interface. The possible reasons for this observation are discussed in the next section. In spite of the differences described above, the most important result of this analysis is that the vibrational population relaxation and long time reorientation dynamics at the interfaces of AOT reverse micelles and lamellar structures are the same within experimental error.



**Table 2.** Interfacial Water Fraction,  $a$ , and Wobbling Fraction,  $b$ , versus Frequency

	2619 $\text{cm}^{-1}$		2609 $\text{cm}^{-1}$		2599 $\text{cm}^{-1}$		2589 $\text{cm}^{-1}$		2578 $\text{cm}^{-1}$	
	$a$	$b$	$a$	$b$	$a$	$b$	$a$	$b$	$a$	$b$
$w_0 = 46$	0.19	—	0.18	—	0.17	—	0.15	—	0.13	—
$\lambda = 46$	0.42	0.39	0.41	0.36	0.38	0.32	0.35	0.31	0.32	0.26
$w_0 = 37$	0.20	—	0.19	—	0.17	—	0.16	—	0.14	—
$\lambda = 37$	0.39	0.40	0.38	0.37	0.35	0.34	0.31	0.31	0.27	0.29
$w_0 = 25$	0.35	0.30	0.34	0.30	0.32	0.30	0.29	0.25	0.25	0.23
$\lambda = 25$	0.62	0.41	0.58	0.37	0.54	0.36	0.48	0.33	0.43	0.29
$w_0 = 16.5$	0.50	0.34	0.49	0.31	0.46	0.28	0.42	0.25	0.37	0.21
$\lambda = 16.5$	0.70	0.39	0.67	0.36	0.63	0.33	0.58	0.32	0.51	0.30

#### D. Interfacial Topography and Its Affect on Water Dynamics

Though the chemical composition of the interface is the same in the AOT reverse micelles and lamellar structures, the surface topography depends on the packing of the AOT molecules and the curvature of the interface. The concave curvature of a reverse micelle interface allows the sulfonate head groups to pack closely together while still allowing room for the bulky tails. As the reverse micelles become larger, the surface curvature decreases, the steric interactions of the AOT tails increase, and these interactions separate the sulfonate head groups. In the limit of an infinitely large reverse micelle, the surface curvature is zero. The steric effects will dominate, and the packing of the AOT molecules will resemble the situation in AOT lamella. For the AOT reverse micelle sizes studied here, Eicke and Rehak<sup>48</sup> have shown that the surface area per AOT varies quickly from less than 30  $\text{\AA}^2$  for the  $w_0 = 2$  reverse micelle up to 50  $\text{\AA}^2$  at  $w_0 = 15$ . After this point, the changes in surface area per AOT are relatively small, approaching a limiting value of 54  $\text{\AA}^2$  by  $w_0 = 40$ . These changes reflect the changing curvature of the interface with increasing reverse micelle size. Fontell<sup>18</sup> has shown that in AOT lamellar structures the surface area per AOT is 65  $\text{\AA}^2$  and is relatively independent of water layer thickness. The difference in surface area per AOT molecule in these two systems requires that we consider how the surface topography and water penetration in the AOT head group region affects the water/interface interactions. Infrared spectroscopy of the hydrophilic portions of the AOT head group can provide insight into the specific differences in water/interface interactions that occur in the lamellar structures and reverse micelles.

The anionic sulfonate head group dominates the water/interface interactions in both the AOT reverse micelles and lamellar structures, requiring  $\sim 6$  water molecules for complete solvation.<sup>43,47</sup> Figure 7 shows the infrared spectrum of the symmetric sulfonate stretch. A number of authors have investigated the changes that occur in the sulfonate stretching region with increased hydration for AOT reverse micelles as well as Nafion fuel cell membranes.<sup>68–71</sup> At low hydration levels, there is a high probability of forming a contact ion pair between the anionic sulfonate head group and the counterion. This causes a blue shift and broadening of the sulfonate stretching spectrum as seen in Figure 7a for the  $w_0 = 2$  spectrum that peaks at  $\sim 1050 \text{ cm}^{-1}$ . Increased hydration and/or larger counterions leads to a red shift and narrowing of the spectrum.<sup>69–71</sup> This behavior is the result of increased hydrogen bonding of water molecules to

the sulfonate head groups that partially screens the sulfonate group from the counterion, reducing its polarizing effect on the sulfonate stretch. Comparison of the  $w_0 = 16.5$  and the  $w_0 = 46$  spectra in Figure 7a, which are essentially identical, shows that the sulfonate group is completely hydrated by  $w_0 = 16.5$ , and no further change occurs in the nature of the environment that the sulfonate group experiences with increased reverse micelle size. No similar studies have been conducted on the sulfonate stretching region of AOT when it forms lamellar structures.

Figure 7b shows a comparison of the reverse micelles and lamellar structures that have  $w_0 = \lambda$ . While the environment of the sulfonate groups in the reverse micelles remains constant, changes continue to occur in the lamellar structures. Interestingly, the lamellar structure with less water,  $\lambda = 16.5$ , experiences a greater red shift, peaking at 1044  $\text{cm}^{-1}$  as opposed to the reverse micelle with  $w_0 = 16.5$  that peaks at 1047  $\text{cm}^{-1}$ . This red shift could be due to a surface topography that allows increased hydrogen bonding to the sulfonate groups, or it could be caused by a greater separation or screening of the sodium

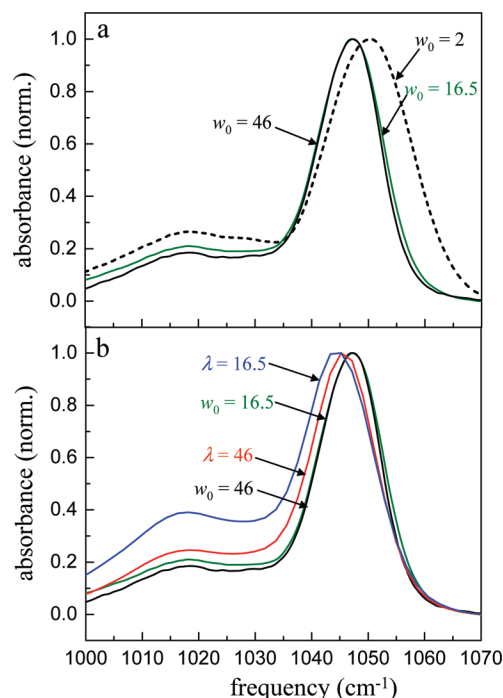


**Figure 7.** Infrared spectra of the symmetric sulfonate stretching region in AOT lamellar structures and reverse micelles. Panel a displays the sulfonate stretch in AOT reverse micelles. Panel b is a comparison of the sulfonate stretch in the largest and smallest reverse micelles and lamellar structures that have  $w_0 = \lambda$ . The sulfonate stretch in the lamellar structures is shifted to lower frequencies than in the reverse micelles. This is attributed to increased separation of the sulfonate group and sodium counterion.

(68) Christopher, D. J.; Yarwood, J.; Belton, P. S.; Hills, B. P. *J. Colloid Interface Sci.* **1992**, *152*, 465–472.

(69) Moran, P. D.; Bowmaker, G. A.; Cooney, R. P. *Langmuir* **1995**, *11*, 738–743.

(70) Moran, P. D.; Bowmaker, G. A.; Cooney, R. P.; Bartlett, J. R.; Woolfrey, J. L. *J. Mater. Chem.* **1995**, *5*, 295–302.

(71) Lowry, S. R.; Mauritz, K. A. *J. Am. Chem. Soc.* **1980**, *102*, 4665–4667.

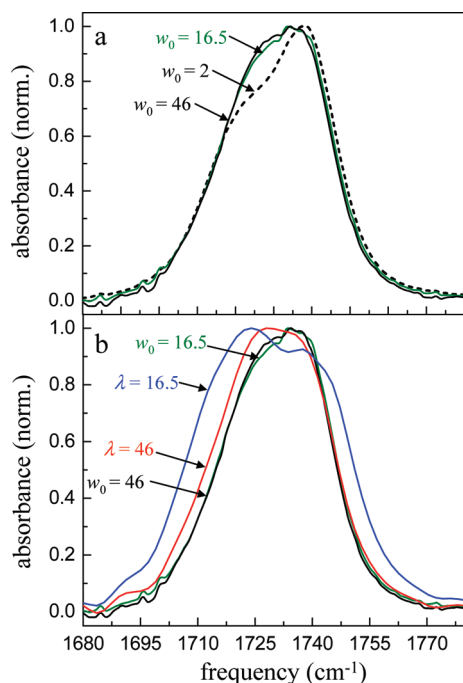


**Figure 8.** Infrared spectra of the ester carbonyl stretching region in AOT lamellar structures and reverse micelles. Panel a displays the carbonyl stretch in AOT reverse micelles. Panel b is a comparison of the carbonyl stretch in the largest and smallest reverse micelles and lamellar structures that have  $w_0 = \lambda$ . The carbonyl stretch in the lamellar structures is broadened and shifted to lower frequencies than in the reverse micelles. The broadening and shift are attributed to increased water and sodium counterion interaction with the ester moiety.

counterion from the sulfonate group for  $\lambda = 16.5$ . In  $\lambda = 16.5$ , the water layer thickness determined by X-ray diffraction is  $\sim 1.6$  nm, which would only accommodate between five and six water molecules between the two surfaces. With such a small volume, entropic effects<sup>72</sup> become important and may drive the sodium counterions out of the water layer into the region behind the sulfonate head groups. This hypothesis is supported by the red shift of the sulfonate stretch and the broadening of the ester carbonyl stretch described below.

In Figure 7, the broad peak at lower frequency,  $\sim 1017$   $\text{cm}^{-1}$ , is probably due to the C–O stretch of the ester group of AOT.<sup>70</sup> This peak was not discussed in previous studies on AOT, but it is not present in the sulfonate stretching region of Nafion, which does not have an ester moiety. The amplitude of this peak does not change significantly in the AOT reverse micelles. However, in the lamellar structures, the peak is greater in amplitude in the red-shifted sulfonate stretch spectrum of  $\lambda = 16.5$  than in the  $\lambda = 46$  spectrum. As discussed further below, the increase in amplitude may indicate greater hydration of the ester group as well as the possibility of increased sodium ion–ester interaction.

Figure 8 shows the ester carbonyl stretching region of the AOT reverse micelles and lamellar structures. The changes in the carbonyl stretching region that occur with increased hydration in AOT reverse micelles have been assigned to rotational isomerization about the acyl C–C bond of the AOT head group that leads to *gauche* or *trans* configurations for the ester carbonyls.<sup>68–70</sup> In the  $w_0 = 2$  reverse micelle, the packing of the AOT molecules allows the more extended *trans* conforma-

tion that peaks at  $\sim 1737$   $\text{cm}^{-1}$  (see Figure 8a). With increased hydration, the decreased curvature of the reverse micelle surface leads to the more wedge-shaped *gauche* conformation,<sup>68</sup> which peaks at  $\sim 1723$   $\text{cm}^{-1}$ . As in the sulfonate stretching region of the reverse micelles, little change occurs in the carbonyl stretching region above  $w_0 = 16.5$ . The opposite is true for the carbonyl stretch in the lamellar structures shown in Figure 8b. At high hydration levels,  $\lambda = 46$ , the carbonyl spectrum is similar to that in the reverse micelles although somewhat broader on the low frequency side. However, the  $\lambda = 16.5$  carbonyl stretching region is dramatically broader with pronounced structure. This broadening of the spectrum with increased amplitude in the lower frequency region has been attributed to interactions between the sodium counterion and the carbonyl group.<sup>69,70</sup> The broadening of the ester carbonyl stretch correlates with the red shifting of the sulfonate stretch and increased amplitude of the peak at  $1017$   $\text{cm}^{-1}$  assigned to the ester C–O stretch for  $\lambda = 16.5$ , providing additional support for the idea that the sodium counterions are being driven out of the center of the water layer to interact more strongly with the ester groups.

The differences in the spectra of the head group moieties in AOT reverse micelles and lamellar structures provide insight into the nature of the water/interface interactions. Whereas the interfacial structure of the AOT reverse micelles remains relatively constant for the larger reverse micelles,  $w_0 > 16.5$ , the structure of the lamellar interface changes considerably. At lower hydration levels, there is significant water penetration past the sulfonate groups in the lamellar structures, leading to increased interactions between the ester moiety, water, and the sodium counterion. The greater surface area per AOT head group in the lamellar structure leads to more water penetration at all hydration levels and increased separation between the sulfonate group and the sodium counterion. These different water/interface interactions explain the larger fraction of interfacial water contributing to the pump–probe signals in the lamellar structures as compared to the reverse micelles that have  $w_0 = \lambda$ .

Although water molecules interact with different groups at the interface in the AOT lamellar structures, the vibrational relaxation and orientational dynamics are very similar. MD simulations of phospholipid bilayers that have similar ester moieties close to the phosphate head group confirm the importance of water/ester interactions for a similar lamellar-type structure.<sup>6,7,73</sup> The time scale for orientational motion of water molecules interacting with the ester groups was estimated at a few tens of picoseconds, in agreement with the results presented here.<sup>6</sup> This result suggests that the specific interactions between water molecules and a hydrophilic surface are not as important as the mere fact that the surface is present.<sup>31,74</sup> A similar conclusion was reached by Moilanen et al. studying the dynamics of water in two reverse micelles of the same size but with different surfactants, nonionic versus ionic.<sup>31,64</sup> This study showed that, for the same size reverse micelle, it was the presence of the interface rather than its nature that determined the water dynamics. The results presented here reinforce this conclusion and further show that the dynamics are dominated by the interactions with the surface rather than a confining length scale. The surface removes some of the normal reorientational

(72) Mitchell-Koch, K. R.; Thompson, W. H. *J. Phys. Chem. C* **2007**, *111*, 11991–12001.

(73) Disalvo, E. A.; Lairion, F.; Martini, F.; Tymczyszyn, E.; Frias, M.; Almaleck, H.; Gordillo, G. *J. Biochim. Biophys. Acta* **2008**, *1778*, 2655–2670.

(74) Scodinu, A.; Fourkas, J. *J. Phys. Chem. B* **2002**, *106*, 10292–10295.

pathways and vibrational relaxation routes that are available to water when it is surrounded completely by other water molecules.

A detailed understanding of the different water/interface interactions that are present in the lamellar structures also allows us to understand the IR spectra more completely. In Figure 2, differences between the IR spectra of the OD stretch in the lamellar structures and AOT reverse micelles only begin to appear at the lower hydration levels, while they are clearly present at all hydration levels in the vibrational lifetime (Figure 3) and the orientational relaxation (Figures 4 and 6) data. The IR spectrum is primarily sensitive to the local electric field and hydrogen bond strength rather than the availability of relaxation pathways. For AOT, the primary source of the blue shift in the OD stretching spectrum is the interaction of water with the sulfonate head groups. Since the sulfonate groups are fully hydrated in both systems, the additional water/interface hydrogen bonding interactions in the lamellar structures may be fairly similar to water–water hydrogen bonds, especially for the high hydration levels,  $\lambda = 46$  and  $37$ . The deviations between the lamellar and reverse micelle OD stretching spectra begin to appear only when the water–ester interactions become more pronounced at the lower hydration levels (see Figure 8), indicating greater water penetration and perhaps water–hydrocarbon interactions that lead to an additional small blue shift in the IR spectrum.

#### IV. Concluding Remarks

We have studied the dynamics of water confined in AOT lamellar structures and reverse micelles to determine the relative importance of confining geometry and nanoscopic length scales versus water/interface interactions. A comparison of lamellar structures and reverse micelles that have the same surface-to-surface distance (lamellar interplanar separation and reverse micelle diameter) shows that the perturbation of water in confined environments is not primarily caused by a specific confining length scale, even when the surface-to-surface distance is  $\sim 1.6$  nm. Instead, the primary factor governing the properties and dynamics of water is the water/interface interactions. The

infrared spectra of the OD stretching mode of water in lamellar structures and reverse micelles that have the same number of water molecules per AOT are virtually the same. However, the vibrational population relaxation appears to be slower for the lamellar structures, and the anisotropy decays appear different, as well. A two-component model was applied to extract the dynamics of the interfacial water for both systems. The results of the two-component analysis show that the vibrational lifetime and orientational dynamics of interfacial water are very similar in the two systems with a characteristic vibrational lifetime of  $T_{\text{int}} = 4.3$  ps and an average orientational time of  $\tau_r^{\text{int}} = 18$  ps. The reason for the apparent slower dynamics in the lamellar structures is that a larger fraction of the confined water molecules are perturbed by the interface. An investigation of the vibrational modes of the AOT head groups provides a rationale for the greater number of perturbed water molecules. In lamellar structures, the surface area per AOT head group is larger, leading to more waters interacting with the head group and increased water penetration past the interface leading to water–ester interactions.

The results presented here provide several key conclusions. First, the perturbation of water by an interface is quite short-range, with substantial alteration of the dynamics of only the water that is directly interacting with the interface. Second, the precise topography of the interface is important but not a dominating factor in determining the dynamical properties of water. The similarity in the long time reorientational dynamics of water in the lamellar structures and AOT reverse micelles indicates that water reorientation is primarily governed by the fact that a surface blocks pathways for new hydrogen bond acceptors rather than the specific hydrogen bonding interactions.

**Acknowledgment.** This work was supported by the Department of Energy (DE-FG03-84ER13251), the National Institutes of Health (2-R01-GM061137-09), and the National Science Foundation (DMR 0652232). D.E.M. thanks the National Science Foundation for a Graduate Research Fellowship, and E.E.F. thanks Stanford for a Stanford Graduate Fellowship.

JA901950B